Multi-scale analysis of snow dynamics at the southern margin of the North American continental snow distribution

CrossMark

Temuulen Sankey *, Jonathon Donald, Jason McVay, Mariah Ashley, Frances O'Donnell, Sharon Masek Lopez, Abraham Springer

Northern Arizona University, 1298 S. Knoles Drive, Flagstaff, AZ 86011, United States

A B S T R A C T

Snow provides a key water source for stream flow and agricultural production across western North America and drinking water for large populations in the Southwest. Accurate estimates of snow cover spatial distribution and temporal dynamics are important at regional and local scales as snow cover is projected to decrease due to global climate change. We examined regional-scale temporal trends in snow distribution across central and northern Arizona using two tiles of 2928 daily images of MOD10 snow product. The analysis included the entire MODIS archive time period, October 1, 2003–June 1, 2014, and a 245,041 km^2 area of 51 HUC8 watersheds. We also examined the effects of a regional forest restoration effort, known as the Four Forest Restoration Initiative (4FRI), aimed at enhancing snow accumulation and retention for increased groundwater recharge through forest thinning and burning treatments. We analyzed 66 Landsat TM/ETM + images spanning 26 years between 1988 and 2014 at five sites and one hyperspectral image from 2014 at two sites. The MOD10 snow product performs well in estimating Arizona's thin and discontinuous snow distribution. Mann-Kendall time-series analysis indicate significantly increasing trends in the annual number of snow cover days (SCD) over the 12-year period in 1.6% of the region at elevation transitions such as the Mogollon Rim in central Arizona, while significantly decreasing trends are observed at a few locations of lower elevations leading to the desert margins in eastern Arizona. The observed temporal trends are mostly consistent with ground-based SNOTEL snow measurements. An Arizona specific, Landsat sensor-derived binary classification model, similar to the MOD10 product, was developed at a local scale. It performs better than commonly-used simple threshold-based approaches, but demonstrates the continued challenges associated with Landsat sensor-derived snow classification in Arizona likely due to its coarse temporal resolution. Landsat-derived multi-temporal Normalized Difference Snow Index (NDSI) analysis indicate that treated (thinned and thinned-and-burned) forest sites had significantly greater NDSI values than untreated control sites. Snowpack at treated sites also appeared to persist longer into the spring season with potentially greater contributions to groundwater recharge in this semi-arid region. The high-resolution hyperspectral data analysis indicate that sites treated to approximately 24% forest canopy cover appear to have an optimum threshold for accumulating and maintaining snowpack. It balances canopy cover versus canopy gap, which reduces snow interception and sublimation by canopy, while providing enough shade. These results are encouraging for the 4FRI, the first and largest forest restoration effort in the US history, aimed at improving watershed health and function in the face of changing climate.

© 2015 Elsevier Inc. All rights reserved.

1. Introduction

Accurate estimates of seasonal snow cover distribution and temporal dynamics are crucial as snow provides a key water source for stream flow (Cayan, 1996; Cayan et al., 1999), agricultural production, and drinking water for much of the global population (Barnett et al., 2005; Dietz et al., 2012). Snow cover in the Northern Hemisphere is one of the key indicators of climate change (Brown, 2000; Intergovernmental Panel on Climate Change (IPCC), 2013). Both the spatial extent and temporal duration of snow cover have been shown to have decreased in the Northern Hemisphere due to warming temperatures and increased climatic variability (Brown, 2000; Brown & Mote, 2009; Dye, 2002; Peng et al., 2013), and are projected to decrease through the 21st century (Adam, et al., 2009; Ashfaq et al., 2013; Brutel-Vuilmet et al., 2013; Mastin et al., 2011). In snow-dominated watersheds of western North America, regional-scale studies have similarly demonstrated decreases in snow accumulation (Barnett et al., 2005; Hidalgo et al., 2009), shorter duration of snow cover (Harpold et al., 2012), decreases in precipitation falling as snow (Knowles et al., 2006), decreases in annual April 1 snow-water equivalent (SWE) in snowpack (Brown, 2000; Mote, 2006),

earlier snowmelt (Barnett et al., 2005; Clow, 2010), decreases in runoff (Stahl et al., 2010), and decreased summer low flows (Stewart, 2009). These effects will likely have an even greater impact on water supply and ecosystem services in the coming decades (Adam et al., 2009; Ashfaq et al., 2013; Intergovernmental Panel on Climate Change (IPCC), 2013).

Winter and spring temperatures in the western US have increased 1 °C over the last 50 years and further 1–2 °C increase is projected by the middle of the century (Intergovernmental Panel on Climate Change (IPCC), 2013). Increasing temperatures are expected to further accelerate the onset of spring and early snowmelt (Harpold et al., 2012; Kapnick & Delworth, 2013; Mote et al., 2005) and decreases in the percent of precipitation falling as snow, which has generated much concern regarding future water supplies (Abatzoglou, 2011; Knowles et al., 2006). In the desert Southwest, these impacts will be coupled with an expected decrease in precipitation due to a northward shift in the mid-latitude storm track (Christensen et al., 2004; Dettinger et al., 1998). Consequently, reduced mountain snowpack will have significant impacts on the Colorado River Reservoir system and the Salt-Verde Watersheds with large implications for water supply and hydroelectric power for southern California and central Arizona metropolitan areas (Barnett et al., 2005) including large cities of Los Angeles and Phoenix with populations of several millions of people. Spring snowmelt, for example, provides approximately 85% of the annual water supply to the Phoenix metropolitan area in central Arizona with a population of 4 million growing at 2.7% per year and expected to reach over 9 million by 2040 (Arizona Department of Water Resources (ADWR), 2010). We examine the effects of regional forest restoration efforts aimed at improved watershed function, which are expected to have significant implications for these large urban populations.

Satellite remote sensing provides the most effective approach to consistently estimating and monitoring spatial and temporal distribution of snow at regional and global scales (Hancock et al., 2013; Rittger et al., 2013). The unique reflective and absorption properties of snow in the visible, near infrared, and shortwave infrared wavelengths make detection by satellite sensors feasible (Dozier, 1984). Satellite-derived global snow products, however, have varying degrees of accuracies and errors (Hancock et al., 2013). Among them, MODIS snow products have been widely employed at a regional scale, with overall accuracies between 90% and 95% (Besic et al., 2014; Hall & Riggs, 2007; Hall et al., 2001a; Huang et al., 2011; Pu et al., 2007; Stroeve et al., 2005; Wang et al., 2008). MODIS (MOD10 Version 5), however, suffers from several sources of snow classification error, including cloud cover, snow cover of less than 10 cm depth, and complex topography that vary substantially within a pixel (Gafurov & Bárdossy, 2009; Hall & Riggs, 2007; Marchane et al., 2015). While the agreement between MODIS binary snow product and ground data is high, previous research indicates it is not sufficient for monitoring snow cover during transition periods (Rittger et al., 2013). More recently, MODIS fractional snow cover products have been developed including MODSCAG (Painter et al., 2009; Arsenault et al., 2012). Continued testing of both the binary and fractional estimates of snow spatial and temporal dynamics are necessary for understanding snow during a time of climatic transition and at spatial transitional zones for snow (Nolin, 2010; Dietz et al., 2012). Of the two MODIS products, we examine here the MOD10 binary snow product in estimating Arizona's highly variable snow distribution. We intend to examine the MODIS fractional snow product in our future studies in Arizona.

Snow cover in Arizona represents the southernmost extent of snow distribution in western North America, where projected decreases in seasonal snow extent are largest (Brutel-Vuilmet et al., 2013). Arizona snow distribution is found at a transition from nearly continuous to ephemeral-mountainous snow cover type with several distinct peaks of accumulation followed by rapid snowmelt within each winter season due to high solar radiation (Ffolliott et al., 1989; Harpold et al., 2012; Molotch et al., 2005). Detection of ephemeral, thin, and discontinuous

snow cover is particularly challenging with coarse-resolution global products such as MODIS (Marchane et al., 2015; Rittger et al., 2013). The large spatial and temporal variability in snow cover across this spatial transition area is further enhanced with a range of topographic, climatic, and hydrological characteristics across central and northern Arizona (Ffolliott et al., 1989). Taken together, the spatial and temporal distribution of snow cover in Arizona provide a unique opportunity to apply, test, and expand upon currently available global snow products and methods.

The spatial and temporal snow dynamics at this transition zone in Arizona are expected to be substantially altered over the coming decades due to a regional-scale forest restoration initiative, known as the Four Forest Restoration Initiative (4FRI), the first and largest restoration effort in the US history to improve forest health (United States Department of Agriculture (USDA), 2013). Through the 4FRI, the U.S. Forest Service plans to conduct forest restoration treatments over a million hectares of Ponderosa pine forest in northern Arizona over the next 20 years to reduce wildfire hazard and improve forest health. One of the 4FRI's key objectives is to thin and burn the forests to create within-stand openings that "promote snowpack accumulation and retention which benefit groundwater recharge and watershed processes at the fine (0.5–5 ha) scale" (United States Department of Agriculture (USDA), 2013). Accurate estimates and monitoring of these expected effects on snow cover are crucial in providing timely information for regional water management and adaptive restoration objectives. Currently lacking is a multi-scale and multi-temporal remote sensing assessment to determine if snow accumulation indeed is greater in treated forests compared to untreated sites and as a result snow persists longer into the spring season in restored forests (Ffolliott et al., 1989; Harpold & Molotch, 2013).

Forest canopy cover substantially impacts snow accumulation by intercepting up to 60% of annual snowfall and sublimating up to 40% of the snowfall in the canopies (Andreadis et al., 2009). As forest canopies are mechanically thinned or burned, much of this effect is expected to be reduced (Varhola et al., 2010 and references therein) leading to increased snow accumulation on the ground and changes in the timing of snowmelt (Gottfried & Ffolliott, 1980). However, these effects are not often quantified at watershed scales (Ffolliott et al., 1989) and integrated into land surface process models (Andreadis et al., 2009). Leveraging three different image sources, we present here regional-scale analysis of spatial and temporal variability of snow cover across central and northern Arizona as well as local-scale, finer-resolution analysis of snowpack and retention following forest restoration treatments. Our objectives were to: 1) assess MODIS data product MOD10 Version 5 (500 m resolution) in daily estimates of Arizona snow spatial variability at a regional scale and evaluate the temporal trend in seasonal snow cover days over the entire MODIS archive time period of 2003–2014, 2) assess multi-temporal Landsat-derived (30 m resolution) snow indices at a local scale to determine snow accumulation changes due to forest treatment and develop an Arizona-specific snow classification model, and 3) determine the optimum ponderosa pine forest canopy cover for snow accumulation and persistence into the spring season using a high-resolution (25 cm resolution) hyperspectral data at forest stand scale in northern Arizona.

2. Methods

2.1. Regional study area description

Our regional-scale analysis was performed across all of central and northern Arizona, USA (Fig. 1). The study region encompasses an approximate area of 245,041 km^2 of the Colorado Plateau and central highlands of AZ spanning an elevation gradient from 450 m in central AZ to 3850 m in northern AZ. The vegetation types along this elevation gradient are chaparral shrublands, high desert grasslands, pinyon–juniper woodlands, ponderosa pine forests, and mixed conifer forests.
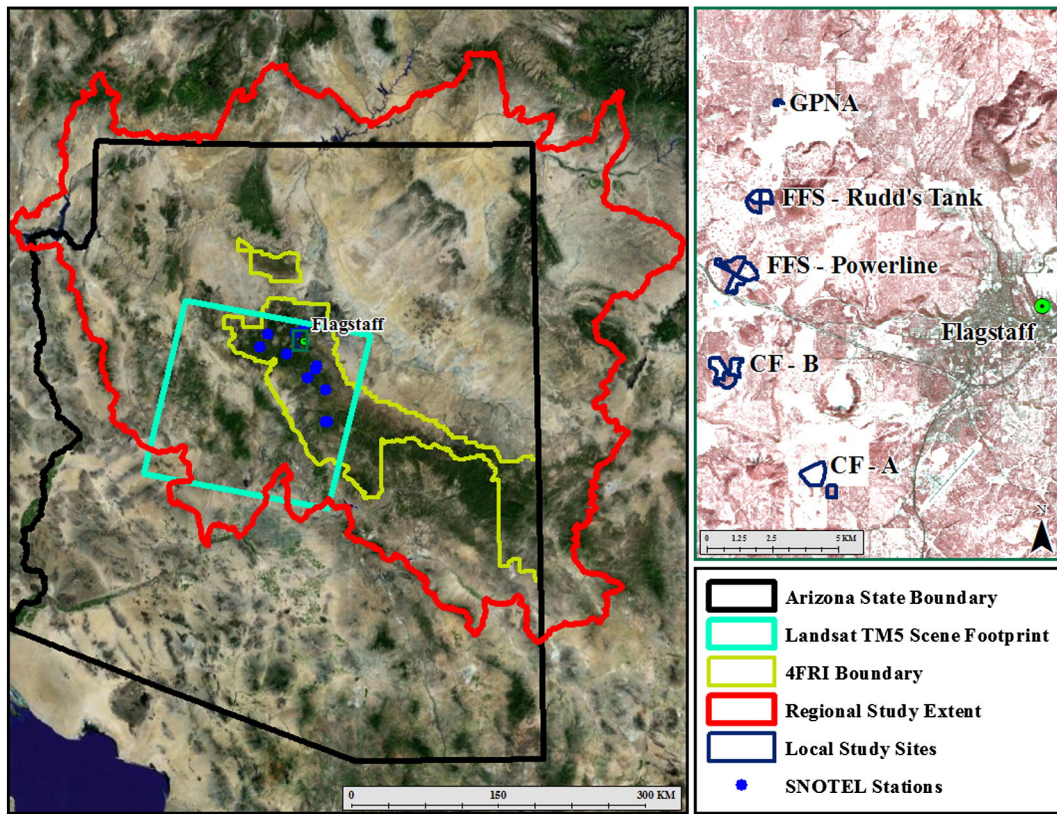
Fig. 1. Study areas included in the regional (panel on the left) and local (panel of the right) scale analysis in AZ. The regional scale analysis included 243,913 km² area in central and northern AZ. Five study areas within the vicinity of Flagstaff in northern AZ are included in the local scale analysis (a green rectangle inside the Landsat image footprint). Each site has three treatments: control, thin, and thin-and-burn, similar to those that will be conducted in the regional forest restoration effort known as the 4FRI.

Average temperature across the study region ranges from 22 °C at low elevations to 2 °C at high elevations. Average annual temperature in this region is believed to have increased 1.5–2.3 °C over the last ~80 years (Jardine et al., 2013; Murphy & Ellis, 2014). Average annual precipitation is ~440 mm across the region with bi-modal peaks in winter and summer.

A total of 51 US Geological Survey Hydrologic Unit Code (HUC8) watersheds were included in this study mostly representing the Upper and Lower Colorado hydrological regions (Table 1). Watersheds that are largely in AZ, but are partially in the neighboring states of southern Utah, southern Nevada, southwestern Colorado, and western New Mexico were also included. The watersheds in Arizona covered 243,913 km² of northern and central Arizona comprising 73.3% of the study region, while the remaining watershed components covered 65,050 km² or 26.6% of the entire study region.

The study region also included a total of 21 microclimate Snow Measurement Telemetry (SNOTEL) Stations established by the Natural Resources Conservation Service (NRCS), USDA. Of the 21 SNOTEL sites, 16 are standard sensors and 5 are enhanced sensors. The standard sensors automatically record daily SWE, snow depth, daily precipitation, and daily minimum, maximum, and average temperature, whereas the enhanced sensors also record soil moisture and temperature at belowground depths of 10, 20, and 50 cm. This information is freely available and reported multiple times a day in near real time (NRCS, 2015). The daily SNOTEL records can be compared to daily remote sensing data products such as the MODIS snow cover map. Some of the sites in the NRCS SNOTEL network cover a long time period dating back to 1978, while others were established more recently. A total of 16 SNOTEL site records in the study region date back as far as the initial date, 2003, of the MODIS time-series used in this study (Table 2).

2.2. Local study area description

Our local-scale analysis focused on the high elevation ponderosa pine forests in the vicinity of Flagstaff, AZ (Fig. 1). Five study sites (Table 3), adjacent to each other, were chosen for more in-depth and finer-resolution analysis (30 m and 20 cm) of snowpack changes due to forest treatments. The five sites were part of small experimental treatments, where ponderosa pine forest has been thinned and thinned-and-burned to test ecosystem function responses to various tree patterns and densities (Table 3) (Dore et al., 2010, 2012; Finkral & Evans, 2008; Kolb et al., 2009; McDowell et al., 2006; Skov et al., 2004; Sullivan et al., 2008). Each study site includes three different treatment units: control, thin, and thin-and-burn (Table 3). The treatments are similar to those that will be conducted in the regional restoration effort 4FRI (Fig. 1). The five study sites are located within 5 km of one another and all represent ponderosa pine forests on similar soils and topography under the same climatic conditions (Table 3). Due to the close vicinity, they experience the same storm events and are found within a single Landsat image footprint. All five sites were, therefore, simultaneously examined in all 66 Landsat images.

2.3. MODIS and SNOTEL data analysis

MODIS/Terra Snow Cover Daily L3 Global 500 m Grid, Version 5 dataset MOD10A1 was primarily used for this study. Temporal gaps in the winter season time series were filled with imagery from MODIS/Aqua Snow Cover Daily L3 Global 500 m Grid, Version 5 dataset MYD10A1 (Hall et al., 2006). Snow cover data from both sensors is processed similarly (Hall et al., 2006), although a different SWIR band from each sensor is used. They are here collectively referred to as the MOD10 data product. MOD10, derived from the MODIS sensor aboard both the

Table 1
Watersheds included in the regional-scale analysis.

Watershed name	HUC	State	Area (km²)
Upper Colorado			
Lower San Juan — Four Corners	14,080,201	CO	5216
Middle San Juan	14,080,105	CO	5042
Chinle	14,080,204	NM	10,830
Chaco	14,080,106	NM	11,886
Paria	14,070,007	UT	3713
Lower Lake Powell	14,070,006	UT	7766
Lower San Juan	14,080,205	UT	6107
Lower Colorado			
Marble Canyon	15,010,001	AZ	3769
Grand Canyon	15,010,002	AZ	6614
Moenkopi Wash	15,020,018	AZ	6854
Havasu Canyon	15,010,004	AZ	7699
Lower Little Colorado	15,020,016	AZ	6244
Hualapai Wash	15,010,007	AZ	4010
Dinnebito Wash	15,020,017	AZ	1933
Corn-Oraibi	15,020,012	AZ	2225
Polacca Wash	15,020,013	AZ	2818
Big Chino-Williamson Valley	15,060,201	AZ	5618
Cottonwood Wash	15,020,011	AZ	4183
Jadito Wash	15,020,014	AZ	2707
Big Sandy	15,030,201	AZ	5562
Middle Little Colorado	15,020,008	AZ	6431
Upper Verde	15,060,202	AZ	6495
Canyon Diablo	15,020,015	AZ	3136
Leroux Wash	15,020,009	AZ	2100
Burro	15,030,202	AZ	1855
Lower Puerco	15,020,007	AZ	2912
Santa Maria	15,030,203	AZ	3754
Chevelon Canyon	15,020,010	AZ	2199
Agua Fria	15,070,102	AZ	6351
Lower Verde	15,060,203	AZ	5092
Hassayampa	15,070,103	AZ	3806
Silver	15,020,005	AZ	2467
Tonto	15,060,105	AZ	2712
Upper Salt	15,060,103	AZ	5612
Carrizo	15,060,104	AZ	1833
White	15,060,102	AZ	1671
Black	15,060,101	AZ	3271
San Carlos	15,040,007	AZ	2760
Upper Gila — San Carlos Reservoir	15,040,005	AZ	7254
Upper Puerco	15,020,006	NM	4982
Zuni	15,020,004	NM	7172
Upper Little Colorado	15,020,002	NM	4200
Carrizo Wash	15,020,003	NM	5805
Little Colorado Headwaters	15,020,001	NM	2041
San Francisco	15,040,004	NM	7267
Upper Gila — Mangas	15,040,002	NM	5385
Lower Virgin	15,010,010	NV	5442
Grand Wash	15,010,006	NV	2426
Lake Mead	15,010,005	NV	7215
Kanab	15,010,003	UT	6160
Fort Pierce Wash	15,010,009	UT	4443

Terra and Aqua satellites (Hall et al., 1995; Hall et al., 2006), includes daily snow cover, snow albedo, and fractional snow cover at 500 m resolution (Hall et al., 2006). Only the MOD10 daily, binary snow cover product was used in this study. The MOD10 snow cover is determined through several criteria: 1) Normalized Difference Snow Index (NDSI) ($(\lambda_{0.6} - \lambda_{1.6}) / (\lambda_{0.6} + \lambda_{1.6})$) greater than 0.4, 2) MODIS band 2 reflectance greater than 0.11, and 3) MODIS band 4 reflectance greater than 0.10 (Hall et al., 2001b). NDSI values less than 0.4 are further tested against NDVI values to determine snow cover in forested areas (Riggs et al., 2006). The MOD10 data product overall accuracy is assessed at 93% and the errors are commonly associated with discriminating snow versus cloud. The MOD10 data product can be acquired in 1200 × 1200 tiles (National Snow and Ice Cover Data, 2015).

We acquired two tiles (H08V05 and H09V05) of daily MOD10 data (http://nsidc.org/index.html) for a total of 2928 days between October 1, 2003 and June 1, 2014. The images were: 1) transformed to UTM projected coordinate system (Zone 12) with NAD 83 datum, 2) mosaicked to combine the two tiles, 3) spatially subset to the study region boundary, and 4) temporally subset to annual snow seasons from October 1 to June 1. This resulted in 12 complete annual snow season image stacks with 244 daily images per year. Within each annual image stack, we summed the number of snow cover days (SCD) for each pixel, which is equivalent to the number of days in a given year when the pixel was classified as snow presence in the MOD10 product. This created a single snow season "image". Each snow season image had a small number of missing snow pixels as the MOD10 product was cloud-filtered and potentially excluded snow pixels, if they were classified as cloudy. We then correlated the MODIS-derived SCD to the ground-based SNOTEL measurements of annual SCD (days with SWE > 0) across the study region. We also stacked together the 12 snow season images to create a final time-series dataset.

A Mann–Kendall rank correlation trend test (MK) was used to determine the existence and magnitude of monotonic trend in each pixel of the final MODIS SCD time-series dataset as well as the winter season-summed SNOTEL station SCD. The MK test is often used to understand the direction and magnitude of trend, as well as the significance of that trend in environmental data (Helsel & Hirsch, 2002; Neeti & Eastman, 2011). The MK tau (τ) coefficient (Eastman et al., 2009; Kendall, 1948; Mann, 1945) is a non-parametric hypothesis test for statistical dependence of observations from two random variables X and Y. Applied to a time series, Y is the temporal component of the time-series data and X in this case is the SCD estimated for each MODIS cell. MK τ ranges from −1 to 1, where positive coefficients indicate an increasing trend, while negative coefficients indicate a decreasing trend. A τ coefficient near zero indicates absence of a trend. An associated two-tailed p-value is an indicator of the trend significance. MODIS cells in which there was no snow for at least half of the time series (6 years) were excluded from the analysis to identify trends in locations with consistent seasonal snow cover. MK has been used frequently in recent years (Czerwinski et al., 2014; de Jong et al., 2011; Gao et al., 2012; Li & Guo, 2012). It is well suited for environmental data: it is resistant to outliers (Neeti & Eastman, 2011; Neeti et al., 2012), performs well with small sample sizes (Yue & Wang, 2004), and does not assume a normal distribution of data (Neeti & Eastman, 2011).

2.4. Landsat-derived binary snow map

We acquired a total of 66 Landsat ETM + and TM images (US Geological Survey Earth Explorer) spanning a 26-year time period from 1988 to 2014. All images were: 1) corrected for atmospheric effects using the FLAASH module in ENVI software (ENVI Version 4.8. ITT Visual Information Solutions, 2010, Boulder, CO), and 2) projected in UTM Zone 12 N, NAD 1983 projection and datum. Using each image, two indices were calculated and combined together: 1) Normalized Difference Vegetation Index (NDVI), and 2) Normalized Difference Snow Index (NDSI). The NDSI was calculated using bands 2 (0.52–0.60 μm) and 5 (1.55–1.75 μm) with the following equation (Dozier, 1989):

$$\text{NDSI} = \frac{\rho_{\text{green}} - \rho_{\text{SWIR}}}{\rho_{\text{green}} + \rho_{\text{SWIR}}}.$$

A threshold value of greater than 0.4 is typically used to distinguish snow from cloud and bright soils and rocks, although NDSI values range from −1 to 1 (Dozier, 1989). In our study area of thin snow cover, a uniform NDSI threshold of 0.4 appeared to underclassify snow in some areas. To produce a binary snow presence and absence map, two different NDSI thresholds were first tested: 0.4 and 0.0. Pixels with NDSI values below the thresholds were classified as snow absence, while all other pixels were classified as snow presence. Klein et al. (1998) modified the 0.4 NDSI threshold using an NDVI adjustment to take into account forest canopy effects on snow detection. This approach was further improved with a spatial correction factor for eastern Canada

Table 2
Characteristics of the SNOTEL sites included in the regional-scale analysis.

Site name	Start date	Latitude	Longitude	Elevation (m)	County	HUC8
Baker Butte	Oct., 1978	34.46	−111.41	7300	Gila	Pine Creek
Baldy	Oct., 1978	33.98	−109.50	9125	Apache	Hall Creek
Beaver Head	May, 1994	33.69	−109.22	7990	Greenlee	Upper Beaver Creek
Coronado Trail	Dec., 1978	33.80	−109.15	8400	Apache	Tsaile Creek–Tsaile Lake
Fort Valley	June, 2008	35.27	−111.84	7350	Coconino	Pitman Valley–Scholz Lake
Fry	Oct., 1978	35.07	−111.84	7200	Coconino	Fry Canyon
Hannagan Meadows	Nov., 1978	33.65	−109.31	9020	Greenlee	Upper Beaver Creek
Happy Jack	June, 1999	34.75	−111.41	7630	Coconino	Brady Canyon
Heber	Aug., 1979	34.31	−110.75	7640	Coconino	West Fork Black Canyon
Maverick Fork	Oct., 1978	33.92	−109.46	9200	Apache	Upper West Fork Black River
Mormon Mountain	June, 2008	34.94	−111.52	7500	Coconino	Mormon Lake
Promontory	May, 1980	34.37	−111.01	7930	Coconino	Upper Willow Creek
Snowslide Canyon	Sep., 1997	35.34	−111.65	9730	Coconino	Bear Jaw Canyon
White Horse Lake	Oct., 1978	35.14	−112.15	7180	Coconino	Upper Hell Canyon
Wildcat	July, 1984	33.76	−109.48	7850	Greenlee	Centerfire Creek
Workman Creek	Oct., 1978	33.81	−110.92	6900	Gila	Workman Creek

(Chokmani et al., 2010) to increase snow detection in forested areas due to Landsat TM NDSI snow underestimates. The spatial correction factor leverages regression relationships between the NDSI and NDVI bands (Chokmani et al., 2010) to also take into account canopy impacts. To increase our snow presence/absence classification accuracy, the spatial correction factor was first tested at our study sites in AZ. The same regression relationship as proposed by Chokmani et al. (2010) was observed at our study area. However, the regression coefficients were different at our study area.

We, therefore, developed an Arizona-specific spatial correction factor as the NDSI-NDVI correlation was unique at our study sites compared to the previously proposed models (Fig. 2). The Arizona-specific model included three steps: 1) All pixels greater than or equal to a NDSI value of 0.4 were classified as snow presence; 2) The relationship between NDSI and NDVI estimates was defined using a linear regression approach (Fig. 2). The regression model was then fit to each of the 66 images. All pixels that fell below the regression line and had NDSI < 0.4 were classified as snow absence, while all pixels above the regression line with NDSI < 0.4 were classified as snow presence. This step added pixels that had NDSI < 0.4 into the snow presence class depending on the NDVI value; and 3) Pixels that were added in Step 2 as snow presence were further filtered using the quadratic regression curve or "the acceptance zone" established by Klein et al. (1998) for NDSI and NDVI (Fig. 2). All pixels that fell below the quadratic regression curve that were classified as snow in Steps 1 and 2 were classified as snow, whereas all other pixels were classified as snow absence. The accuracy of this model was assessed using daily measurements from SNOTEL sites that matched the Landsat image dates.

### 2.5. Landsat-derived NDSI in assessing forest restoration effect

We correlated the Landsat-derived NDSI values to the SNOTEL snow depth measurements including the Fort Valley SNOTEL station (significance level $p = 0.05$ at 95% confidence interval). As a surrogate estimate

of snow accumulation, the NDSI values from all 66 images were compared among the restoration treatment units at all study sites via an analysis of covariance (ANCOVA) test, in which treatments and sites were used as factorial variables and image dates as a covariate. In addition, pre-treatment mean NDSI values were calculated for each pixel across all pre-treatment years (Table 3) and examined using an analysis of variance (ANOVA) with Tamhane's post hoc multiple comparisons. To evaluate the forest restoration treatment effects, changes in NDSI values were estimated by differencing the mean NDSI values from all pre-treatment years versus all post-treatment years for each pixel (Table 3) and compared using an ANOVA test. Similar analysis was performed with Landsat-derived Normalized Difference Vegetation Index (NDVI) using all 66 images. Pre-treatment mean NDVI values were first analyzed to determine if differences in ponderosa pine forest conditions existed prior to treatment. Mean changes in NDVI values following treatment were then estimated and compared to determine if forest restoration treatments further enhanced differences in ponderosa pine forest conditions and achieved the stated goals of the regional restoration efforts.

The NDSI values from 17 images at the end of the snow season from March 1-April 1 were compared at the treated versus untreated control sites to evaluate the effects of the forest restoration treatments on snow retention and persistence into the spring season. In addition, NDSI values from treated versus untreated control units from the winter season of 2009–2010 were examined at a higher temporal resolution, because: 1) treatments at all sites were completed by this season (Table 3), 2) a total of 13 cloud-free Landsat images were available over this single season (Oct. 29, 2009; Nov. 30, 2009; Dec. 8, 2009; Dec. 24, 2009; Jan. 9, 2010; Jan. 17, 2010; Jan. 25, 2010; Feb. 18, 2010; Feb. 26, 2010; March 6, 2010; March 14, 2010, March 22, 2010, and March 30, 2010), while all other seasons had <5 images/season, and 3) the last available image date of the season was March 30, 2010, which closely matches to the commonly used April 1 date for annual cumulative snowpack (Brown, 2000; Mote, 2006; Varhola et al., 2010).

Table 3
Characteristics of the five study sites included in the local-scale analysis. Site exposure index was calculated using topographic slope and aspect to rescale aspect to a north–south axis integrated with the steepness of the slope (Balice et al., 2000).

Treatments	Total area (ha)	Treatment Year	Avg slope (degree)	Site exposure index	Elev. (m)	Avg annual precipitation (mm)	Avg annual temp (C)	# images pre-treatment	# images post-treatment
Gus Pearson Natural Area	3.53	1993	1.5	−0.2	2240	590	6.9	5	61
Rudd's Tank	53.31	2003	2.0	0.8	2270	590	6.9	28	38
Powerline	97.79	2003	2.1	0.8	2249	581	7	28	38
Centennial Forest — B	71.04	2003	2.7	0.6	2254	571	7.1	28	38
Centennial Forest — A	83.42	2006	3.6	1.7	2186	560	8	35	31

$$Y = -0.18 + 4.75X - 4.5X^2$$
$$Y = 0.23 - 0.18X$$
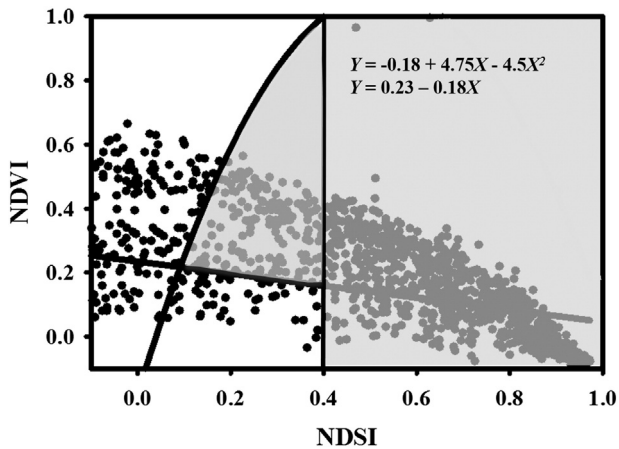
Fig. 2. Arizona-specific snow classification model using Landsat-derived NDSI and NDVI. Pixels in the highlighted areas were classified as snow and met one of two criteria: 1) NDSI > 0.4; or 2) pixels above the linear regression line, but below the quadratic regression line. All other pixels were classified as snow absence.

2.6. Hyperspectral image analysis

We analyzed a hyperspectral image to determine the optimum forest canopy cover which supported the most persistent snow retention observed in the Landsat imagery into the spring season. The hyperspectral image was acquired in October, 2014, in 272 spectral bands (397–1002 nm) and 25 cm resolution using a Headwall Photonic nano-hyperspectral sensor mounted on a Cessna Turbo 206 fixed-wing aircraft. The image tiles were first orthorectified and mosaicked to fully cover two of our study sites, Centennial Forest A and B, where snow accumulation in treated sites was found to be greatest in the multi-temporal Landsat images across all years. The other sites were not included in the hyperspectral image acquisition. Using spectral bands in 670 nm and 800 nm, we calculated NDVI. Using a threshold of NDVI > 0.6 and a segmentation approach in ENVI, we delineated individual tree canopies. A grid with 30 m cells were overlaid on the resulting classification and used to estimate percent canopy cover and tree density within each 30 m cell to correspond to the Landsat NDSI pixels.

3. Results

3.1. MODIS

Approximately a 168,892 km^2 area or 69.2% of the study region (675,567 pixels) was analyzed for temporal trends in MOD10 snow cover days (SCD) (Fig. 3). Within this area, a total of 2650 km^2 area, equivalent to 1.6% of the study region (10,600 pixels), had significant trends (p < 0.05). Of these, 2544 km^2 (10,176 pixels; 96% of the significant trend area) showed significantly increasing trends, while 106 km^2 (424 pixels; 4% of the significant trend area) had significantly decreasing trends in the number of SCD over the 12-year study period. The significantly increasing number of SCD areas overlapped with several SNOTEL stations, which also indicated an increasing trend over the 12-year study period (Fig. 4) with slope coefficients significantly different from 0. The MODIS-derived number of SCD correlation coefficient (R) with SNOTEL SCD was 0.80 with a significant p-value of 0.001 (adjusted R^2 = 0.62) (Fig. 5), when all SNOTEL sites were combined. The degree of correlation varied across the SNOTEL sites, when 16 SNOTEL sites with matching 12-year records were individually examined (Table 4). The MODIS-estimated number of SCD was significantly correlated at all SNOTEL sites except at Workman Creek and Snowslide Canyon sites (p-values of 0.146 and 0.939, respectively) (Table 4).

3.2. Landsat-derived binary snow cover

A total of 10 SNOTEL site locations overlapped with the Landsat scene footprint with a total of 459 matching daily measurements in the 66 images. These measurements were converted into binary values of snow presence and absence to assess the accuracy of the Landsat-derived classification (Table 5). The commonly used NDSI thresholds of 0.4 and 0.0 produced overall accuracies of 77% and 90%, respectively, with low accuracies for snow absence. The Landsat-derived binary classification with the Arizona-specific model produced an overall classification accuracy of 86% (Table 5). While producer's accuracy improved for snow absence in this model, user's accuracy remained low. This appeared to be due to several dates when traces of snow were monitored at the SNOTEL stations after snowmelt following a storm, but no detectable snow was observed in the Landsat pixels. When the commonly used <10 cm threshold (Marchane et al., 2015) snow dates were removed, user's accuracy for snow presence remained at 96%, but user's accuracy for snow absence improved to 67%. This model produced the best overall accuracy of 91%.

3.3. Landsat-derived NDSI estimates and treatment effects

SNOTEL snow depth measurements from the 459 matching dates to the 66 Landsat image dates were significantly correlated to the Landsat-derived NDSI values (p-value = 0.000; R = 0.48). The degree of correlation varied across the ten SNOTEL sites when they were individually examined (Table 6), although the relationship was always significant except at the Chalender site (p-value = 0.126, Table 6). Particularly, at the Fort Valley site, the SNOTEL snow depth measurements were significantly correlated with the Landsat-derived NDSI values (p-value < 0.001; R = 0.763).

Following treatment, previously existing NDVI differences were enhanced: NDVI decreases at all treated units were significantly greater compared to the respective control units (all p-values < 0.001) (Fig. 6). Furthermore, the mean NDVI decrease at thin-and-burn treatment units were significantly greater than their thin treatment counterparts (all p-values < 0.01), except at the Gus Pearson National Area (GPNA) and Rudd's Tank (p-values of 1.00) (Fig. 6).

NDSI comparisons indicated that forest treatments had significant effects (p < 0.001), along with image dates (p < 0.001), on NDSI, but site was not a significant variable (p = 0.247). Consistent with the NDVI trends, the mean NDSI values were significantly different prior to treatment at many of the sites. Landsat-derived NDSI values were already significantly greater in the thin treatment units of the Centennial Forests A and B (both p-values < 0.000) compared to the control units. NDSI values were also significantly greater within the thin-and-burn treatment unit at Rudd's Tank site compared to its control and thin treatment units (p-values < 0.001). However, no significant differences were observed among the treatment units at the GPNA site prior to treatment and NDSI values were significantly lower in the thin-and-burn unit of the Powerline site and Centennial Forest B site.

Following treatment, significant increases in mean NDSI values were observed at all of the treated units. NDSI increases in thin and thin-and-burn treatments were both significantly greater compared to the control treatment at all four sites (all p-values < 0.01) (Fig. 7). Furthermore, NDSI increase at the thin-and-burn treatments were significantly greater compared to the thin treatment at the Rudd's Tank and Centennial Forest B sites (both p-values < 0.001) (Fig. 7). The increased NDSI following treatment also appeared to persist longer into the spring season. Mean NDSI values at the end of the winter season were significantly greater (all p < 0.001) at all treated sites compared to the control sites in all of the 17 image dates examined. Furthermore, over the winter season 2009–2010, NDSI in control and treatment units similarly fluctuated, but treated units had consistently greater NDSI throughout the season. More importantly, at the end of the winter season on March
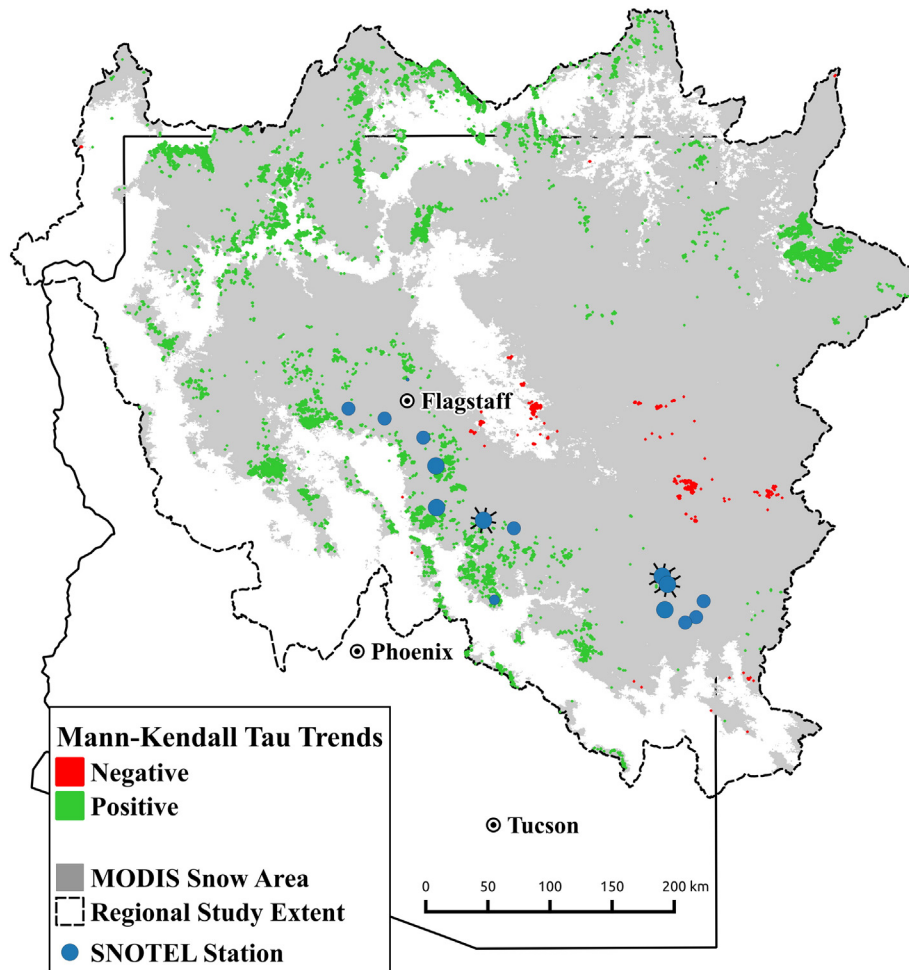
Fig. 3. The trends observed in the MODIS-derived number of snow covered days (SCD) within each pixel across the study region in AZ over the 12-year study period (white areas show pixels removed due to consistent snow absence). Locations where the observed trends were significant are highlighted in red (negative trend) and green (positive trend). The MODIS-derived SCD are consistent with ground-based SNOTEL measurements (blue circles) of SCD over the same period (degree of agreement indicated by the size of the circles) (Table 4). Similar to the MODIS-derived SCD, the ground-based SNOTEL measurements indicate that SCD over the 12-year period is increasing at some locations in Arizona, although SCD shows generally decreasing trend over a longer time period of the last several decades (Fig. 4). SNOTEL locations shown in Fig. 4 are highlighted here with asterisks around the blue dot. (For interpretation of the references to color in this figure legend, the reader is referred to the web version of this article.)

30, 2010, treated units had consistently greater NDSI compared to their control counterparts (Fig. 8) (p-values < 0.01).

In particular, the increased snow accumulation at the treated units of Centennial Forest A and B sites persisted longer following the snow season of 2009–2010 (Fig. 8). Although NDSI similarly fluctuated at these sites throughout the season, the treated units had consistently greater NDSI at the end of the snow season by April 1, 2010 (all p < 0.001).

3.4. Hyperspectral image analysis

Forest canopy cover ranged 22–51% and tree density varied between 7 and 14 trees within the 30 m cells across the entire area covered in the hyperspectral data across the Centennial Forests A and B (Table 7). The Centennial Forest A site had only two treatments: control and thin (Fig. 8, Panel A). The control site had a mean canopy cover of 39.5% and a mean density of 14 trees/cell within the 30 m cells. In comparison, the thin treatment had a mean canopy cover of 22.7% and a mean density of 8 trees/cell within the 30 m cells. The Centennial Forest B site had three treatments: control, thin, and thin-and-burn (Fig. 8, Panel B). The thin and control treatments at this site had 22.4% and 50.9% canopy cover, respectively, and 6 trees/cell and 12 trees/cell tree density, respectively. The thin-and-burn treatment at the Centennial Forest B site had a mean forest canopy cover of 23.9% and a mean tree density of 7 trees/cell. Among the five units at these two sites, the mean Landsat-

derived NDSI was largest at the thin-and-burn site of the Centennial Forest B, which might indicate that 24% forest canopy cover and 7 tree/cell tree density are optimum for snow retention.

4. Discussion

4.1. MODIS-derived snow estimates and trends

MODIS global snow product, MOD10, appears to perform well in Arizona, where snow is thin and patchy with a large spatial and temporal variability. Other MOD10 studies have had to introduce complex correction factors due to cloud cover and snow detection thresholds of 10 cm (Marchane et al., 2015). However, MOD10 generally correlated well with most SNOTEL measurements in our study region. The MOD10-derived number of snow cover days (SCD) underpredicted the SNOTEL-measured SCD by only 2 days, on average, in our study region as indicated by the intercept of the regression model. Other MODIS studies documented large omission errors (60%) when comparing MODIS data to finer-resolution snow estimates and other data sources (Metsämäki et al., 2002; Rittger et al., 2013). In this study, we compare MOD10 data with only SNOTEL stations in Arizona and as a result might have missed potentially large omission errors documented in other studies. The SNOTEL stations with the poorest correlation coefficients and large underestimates of SCD of up to 40 days in our study were
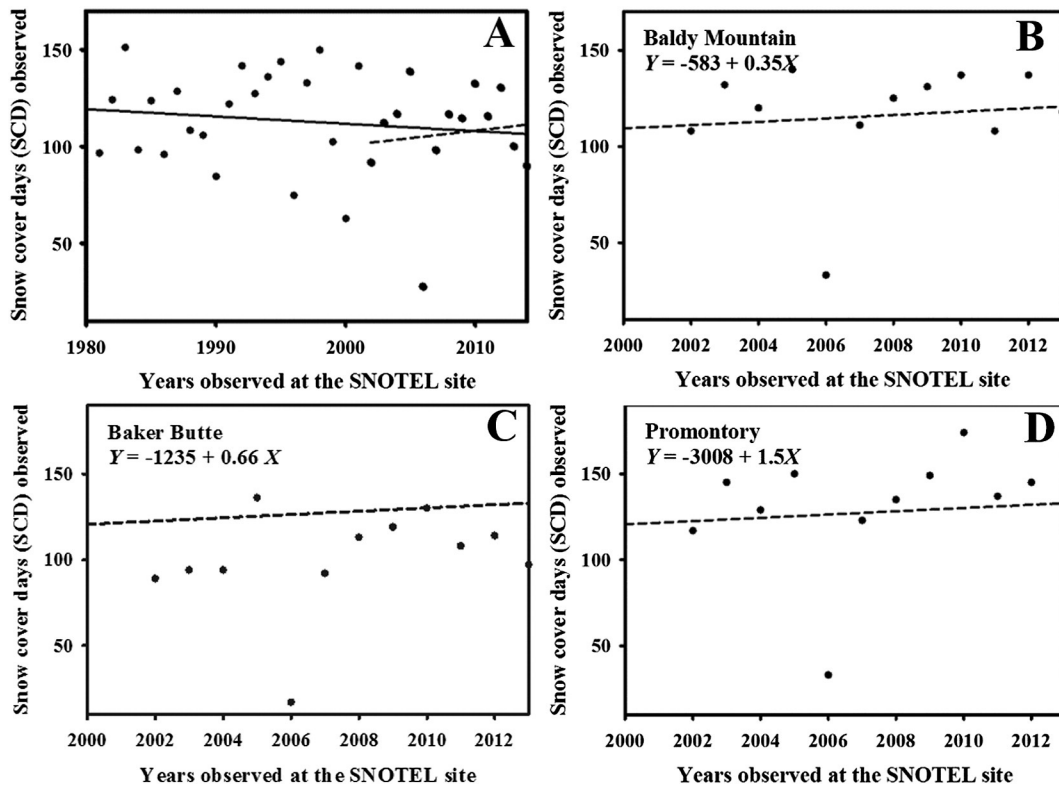
Fig. 4. The temporal trends in the number of snow cover days (SCD) observed: a) across all SNOTEL stations dating back to 1980 (Panel A), where the multi-decadal trend is indicated by a solid line and the trend of the 12-year study period is indicated by a dashed line, b) at the Baldy Mountain SNOTEL station (Panel B) over the study period, c) at the Baker Butte SNOTEL station (Panel C) over the study period, and d) at the Promontory SNOTEL station (Panel D) over the study period.

located in complex terrain where elevation, slope, and aspect were highly variable within a MODIS pixel (500 m), consistent with previous conclusions (Marchane et al., 2015). Taken as a whole, our results extend to the Southwest previous observations of high accuracy of MODIS-derived snow maps over large areas of non-forested, uniform terrain (Hall & Riggs, 2007; Huang et al., 2011; Pu et al., 2007; Salomonson & Appel, 2004), but demonstrated that complex terrain remains to be a challenge (Hall et al., 2001a; Romanov & Tarpley, 2007; Shreve et al., 2009). Future studies in the Southwest can test MODIS fractional snow cover estimates in complex terrain to enhance MOD10-derived snow maps.

This study, to our knowledge, is the first spatially-explicit temporal analysis of snow dynamics across Arizona. We find that the daily temporal resolution of the regional-scale MOD10 product is ideal for Arizona, where each snow season within a single year is characterized by several distinct storm events with snow accumulation followed by rapid snow-melt within a few days (Ffolliott et al., 1989). In the Southwest, MOD10 product further complements daily SNOTEL-based temporal analysis (Harpold et al., 2012; Molotch et al., 2005) since SNOTEL stations only represent point locations distributed sparsely across large areas. The temporal trend agreement between SNOTEL and MOD10 snow product observed in this study is encouraging for consistent snow monitoring in
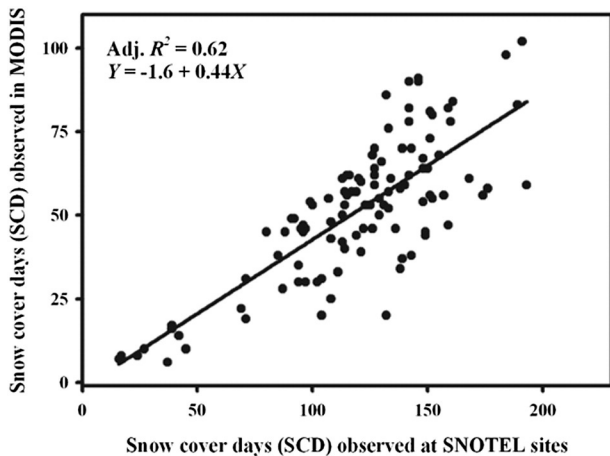

Fig. 5. Relationship between the MODIS-derived and ground-based SNOTEL-derived number of snow cover days (SCD) across our study region.

Table 4
Correlation coefficients in the MODIS-derived and SNOTEL-measured number of snow cover days (SCD) annually over the 12-year study period. SNOTEL sites with fewer than 12-year records were not included. Significant trends in the SNOTEL data are indicated with *.

SNOTEL sites	Correlation coefficient (R)	P-value	Trend indicated by Thielsen's slope
Baker Butte	0.761	0.002	0.663*
Baldy Mountain	0.915	0.000	0.452*
Coronado Trail	0.688	0.007	−0.650
Hannagan Meadow	0.730	0.003	−2.292*
Fry	0.688	0.007	2.000
Happy Jack	0.836	0.000	2.307
Heber	0.707	0.005	0.913*
Maverick Fork	0.881	0.000	−0.041*
Mormon Mountain	0.707	0.005	1.812
Promontory	0.785	0.001	1.606*
White Horse Lake	0.724	0.003	−0.187
Wildcat	0.758	0.002	−0.583*
Beaverhead	0.600	0.023	−2.833
Workman Creek	0.410	0.146	−0.944
Snowslide Canyon	0.023	0.939	−2.467

Table 5

Accuracy assessment of the Landsat-derived binary classification of snow presence and absence. The accuracies of each classification are highlighted in bold.

Classes	Snow absence	Snow presence	Total
Snow absence (NDSI threshold > 0.4)	36	10	46
Snow presence (NDSI threshold > 0.4)	90	306	396
Total (NDSI threshold > 0.4)	126	317	442
Producer's accuracy	**29%**	**96%**	
User's accuracy	**78%**	**77%**	
Overall accuracy			**77%**
Snow absence (NDSI threshold > 0.0)	27	28	55
Snow presence (NDSI threshold > 0.0)	17	371	388
Total (NDSI threshold > 0.0)	44	399	442
Producer's accuracy	**61%**	**93%**	
User's accuracy	**49%**	**96%**	
Overall accuracy			**90%**
Snow absence (AZ-specific model)	29	40	69
Snow presence (AZ-specific model)	12	305	317
Total (AZ-specific model)	41	345	386
Producer's accuracy	**70%**	**88%**	
User's accuracy	**42%**	**96%**	
Overall accuracy			**86%**
Snow absence (AZ-specific model, 0.1 m)	39	39	58
Snow presence (AZ-specific model, 0.1 m)	11	280	291
Total (AZ-specific model, 0.1 m)	50	319	369
Producer's accuracy	**78%**	**93%**	
User's accuracy	**67%**	**96%**	
Overall accuracy			**91%**

Fig. 6. Post-treatment Normalized Difference Vegetation Index (NDVI) decrease at all study areas. All treatment units had significantly greater NDVI decrease compared to the control sites. Thinning treatments and thin-and burn treatments also resulted in significantly different NDVI decreases. Only at Gus Pearson National Area (GPNA), there was no significant difference between these two treatments (indicated by letters). Centennial Forest A site (CF-A) had only control and thin treatment units.
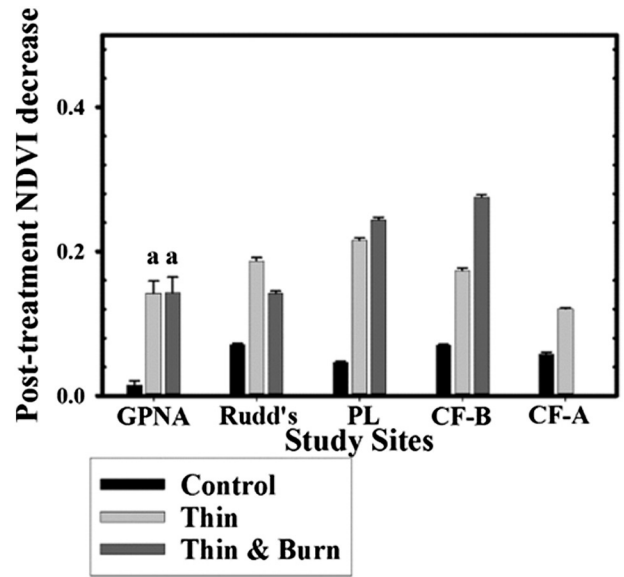
the future at Arizona's ephemeral zone that represents the continental margins of snow distribution, which is most susceptible to global climate change (Brutel-Vuilmet et al., 2013). Trends observed at these margins can inform patterns to be expected in the future throughout the North American continent.

While the trends were spatially variable, MOD10-derived SCD Mann-Kendall trends were predominantly increasing, when significant, across the study region over the 12-year study period. The increasing trends were observed at elevation transitions such as the Mogollon Rim, while decreasing trends were found at lower elevations leading to the desert margins in eastern Arizona (Fig. 3). Interestingly, both of these patterns are found at the topographic transitions surrounding the high elevation area of northern Arizona. A similar magnitude trend of increasing SCD was observed in some of the SNOTEL measurements over the same 12-year period (Fig. 4), consistent with Palmer Drought Severity Index (PDSI) trends for Northern Arizona. Twelve SNOTEL sites used in our study have records extending to the early 1980s, and exhibit trends of decreasing SCD over the multi-decadal time period (Fig. 4), but increasing trends over the recent 12-year period at most sites (Fig. 4). Similar trends still remain at most of these sites even if the anomalous year of 2006 is removed. Climatic modes of Pacific origin such as the El Niño Southern Oscillation (ENSO) and the Pacific Decadal Oscillation (PDO) are strongly correlated with temperature

and precipitation variation across western North America (Barnett et al., 2005; McCabe & Dettinger, 2002; Stoner et al., 2009; Svoma, 2011). The observed upward SCD trends over the 12-year time period is likely driven by the climatic variability at the sub-decadal scales, especially ENSO (Svoma, 2011). Furthermore, it is likely that the contribution of extreme events to snowfall is increasing, replacing more frequent low intensity storms with intermittent storms with greater snowfall (Lute & Abatzoglou, 2014). While such shifts cannot be explicitly examined with the MOD10 product, future temporal trend analysis
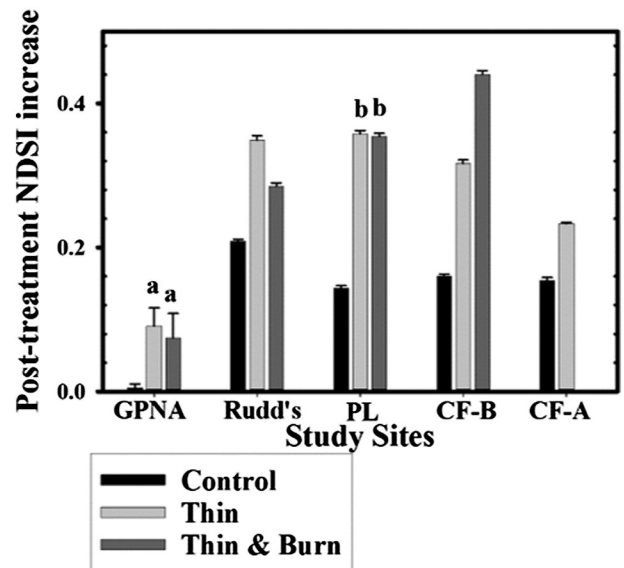
Fig. 7. Post-treatment Normalized Difference Snow Index (NDSI) increase at all sites. All treatment units had significantly greater NDSI increase compared to the control sites. Thinning treatments and thin-and burn treatments also resulted in significantly different NDSI increases at Rudd's Tank, Centennial Forest B (CF-B), and A (CF-A) sites. At Gus Pearson National Area (GPNA) and Powerline (PL) sites, there was no significant difference between these two treatments (indicated by letters). Centennial Forest A site (CF-A) had only control and thin treatment units.
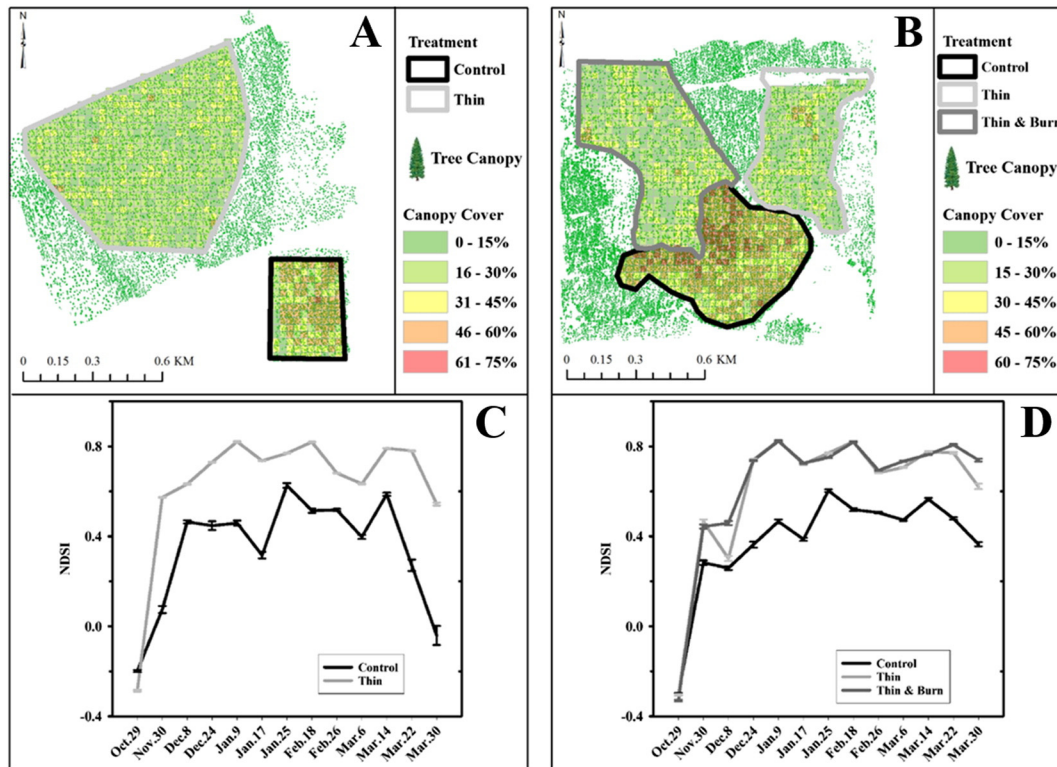
Table 6

Correlation coefficients in the Landsat-derived Normalized Difference Snow Index (NDSI) and SNOTEL-measured snow depth at 10 sites that overlapped with the Landsat scene footprint.

SNOTEL sites	Correlation (R)	P-value	N of matching dates
Baker Butte	0.51	0.000	67
Baker Butte Summit	0.78	0.000	20
Chalender	0.36	0.126	19
Fort Valley	0.76	0.004	27
Fry	0.46	0.000	66
Happy Jack	0.51	0.000	50
Mormon Mountain	0.48	0.000	66
Mormon Mountain Summit	0.60	0.003	26
Snowslide Canyon	0.40	0.003	52
White Horse Lake	0.60	0.000	65

Fig. 8. The two sites (Panels A and B) with consistently the largest NDSI among all sites and post-treatment snow retention (Panels C and D) at control and treated units at the two sites over the winter season of 2009–2010. A total of 13 cloud-free images were available over this season (Panels C and D) and the last image date of March 30, 2013 closely matched April 1, the standardized date for comparison in North America. Thin and thin-and-burn treatments (>100 pixels) had greater NDSI persisting into the spring season at both sites (Panels C and D). Centennial Forest B thin-and-burn site (Panel D) had the largest NDSI at the end of the season and likely represents optimum canopy cover for snow accumulation and retention. A high-resolution (0.25 m) airborne hyperspectral image (Panels A and B) indicates that the forest canopy cover at this site is 24%, which likely has reduced snow interception and sublimation by the forest canopy following treatment, while providing enough shade on the ground.

could address this question using other data sources. The MOD10 time-series data can, however, spatially demonstrate areas of AZ where extreme SCDs are observed, regardless of whether they result from frequent low intensity storms or few large events, over the study period as potentially sensitive areas indicative of future trends. Fig. 9 illustrates areas of very small versus large numbers of SCD across AZ using the lower and upper five percent of the 12-year mean SCD distribution (5th and 95th percentiles, respectively). The very small numbers of SCD are commonly observed across central AZ along the Mogollon Rim below 1800 m elevations including HUC8 watersheds of Big Sandy, Big Chino-Willamson Valley, Lower Verde, Tonto, Upper Salt, and San Francisco. In contrast, the very large numbers of SCD are observed mostly at high elevations above 2300 m in the mountainous northern portions of AZ including HUC8 watersheds of Lower Colorado-Marble Canyon, Lower Little Colorado, Canyon Diablo, Middle Little Colorado, Chevelon Canyon, and Little Colorado Headwaters.

### 4.2. Landsat-derived snow estimates and trends

The Landsat NDSI-derived binary snow presence/absence classification performance was generally low when simple NDSI thresholds of 0.4

(Hall et al., 1995) and 0.0 were applied. The Arizona-specific regression-based classification approach with a modified spatial correction factor resulted in the most balanced producer's and user's accuracies for snow presence and absence. This model was based on a NDSI–NDVI relationship unique to our study area and an integrated concept proposed by Klein et al. (1998) and Chokmani et al. (2010). Other studies have similarly mapped snow with regional adjustments of Landsat NDSI (Maher et al., 2012; Vogel, 2002). Even after integrating NDVI and canopy cover effects, the best performing Arizona-specific model tended to underestimate thin snow cover and benefited from the commonly used 10 cm snow detection threshold (Marchane et al., 2015). Many locations in this semi-arid state can typically receive <10 cm snow, which appears extremely challenging to map. Taken together, these results suggest that mapping thin snow cover remains a challenge with Landsat imagery at Arizona's ephemeral snow transition zone. We attribute much of this challenge to the high temporal variability in Arizona's snow distribution in relation to the coarse temporal resolution of the Landsat data. Over much of the study period, Landsat data were 16 or more days apart. Snow cover in Arizona, however, typically lasts only a few days and rapidly melts after each storm during a snow season. Much of the snow cover is typically melted and snow distribution is

Table 7

Hyperspectral image-derived mean and standard deviation (SD) of tree canopy cover and density estimates within 30 m cells.

Study sites	Canopy cover mean (% in cells)	Canopy cover SD (% in cells)	Density mean (# trees/cell)	Density SD (# trees/cell)
Centennial Forest A: control	39.5%	11.8%	14	4.7
Centennial Forest A: thin	22.7%	7.5%	8	2.9
Centennial Forest B: control	50.9%	9.9%	12	2.9
Centennial Forest B: thin	22.4%	9.6%	6	2.7
Centennial Forest B: thin-and-burn	23.9%	11%	7	3.5
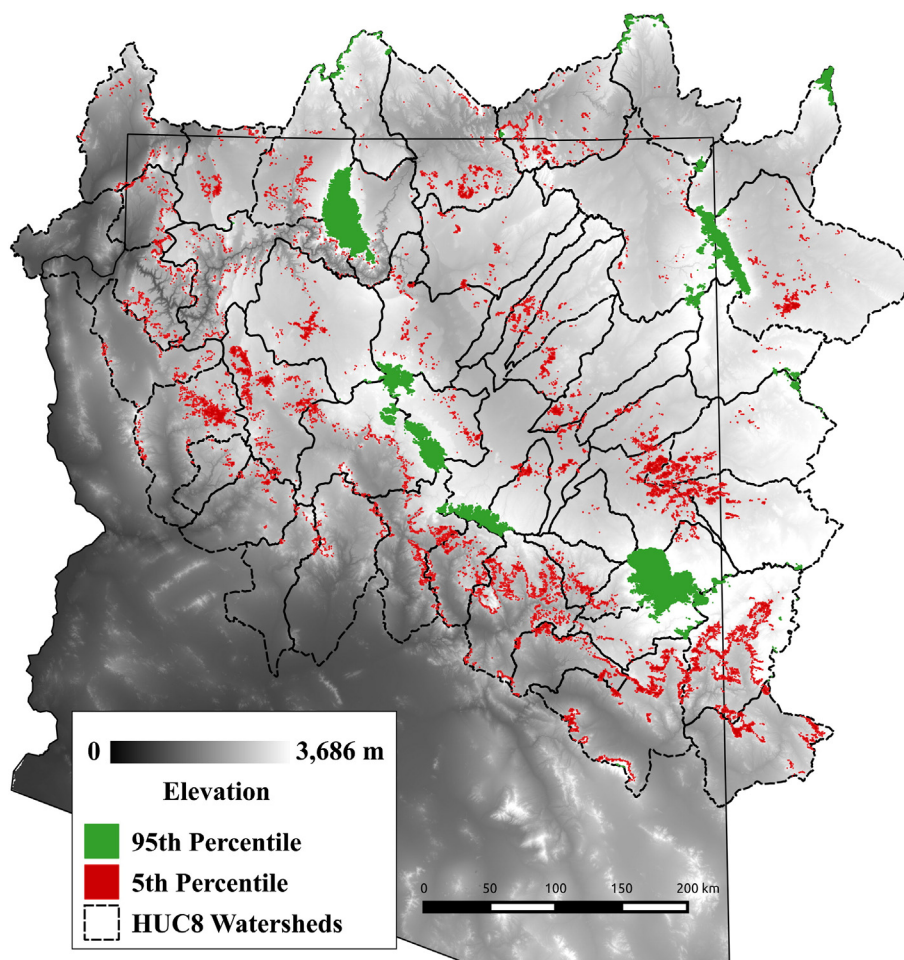
Fig. 9. Spatial distribution of the 5th (red) and 95th (green) percentile of the MODIS-derived 12-year mean SCD across elevation gradients of AZ as potentially sensitive areas indicative of future trends. (For interpretation of the references to color in this figure legend, the reader is referred to the web version of this article.)

spatially patchy, when revisiting a site with Landsat sensors at 16 day intervals. Higher spatial resolution data (Czyzowska-Wisniewski et al., 2015) or higher temporal resolution data such as daily MOD10 better address this aspect of the challenge.

We present here the first multi-temporal Landsat NDSI analysis of snow accumulation following ponderosa pine restoration treatment efforts in Arizona. Landsat NDSI performed well at our local study area ($R = 0.76$; Table 6), where the SNOTEL station could be accurately mapped within a 30 m pixel. Our results indicate that Landsat-derived NDSI values were significantly different among treatment units and depending on image date. In particular, NDSI values were significantly greater following forest restoration treatments at both thin and thin-and-burn treatments at each site. Furthermore, thin-and-burn treatment units had significantly greater NDSI increase compared to their thin treatment counterparts. The increased NDSI at the treated sites were likely due to the lower vegetation canopy cover (Klein et al., 1998; Lundberg et al., 2004). Forest canopy can significantly impact snow accumulation on the ground (Lundberg et al., 2004; Nakai, 1996; Varhola et al., 2010) by intercepting and sublimating up to 40% of snowfall (Lundberg & Halldin, 2001). Previous ground-based studies in other forest types and management treatments have demonstrated that thinned forest canopy cover and density can result in less snow intercepted and, consequently, greater snow accumulation on the ground, snow retention, and snow water equivalent (SWE) (Ffolliott & Baker, 2000; Ffolliott et al., 1989; Hedstrom & Pomeroy, 1998; López-Moreno et al., 2008; Teti, 2008; Varhola et al., 2010; Woods et al., 2006), although very few studies have focused on forest restoration treatments in the Southwest (Heffelfinger, 2012; Varhola et al., 2010). It

is encouraging for the regional forest restoration effort 4FRI that such effects are observed via satellite remote sensing, especially considering its key objective is to increase snow accumulation and retention to enhance groundwater recharge in Arizona. The application of satellite remote sensing at similar scales to the 4FRI restoration effort is especially important, because ground-based measurements such as snow course data often represent small canopy openings that accumulate more snow and cannot be uniformly extrapolated to larger spatial extents (Ffolliott et al., 1989; Varhola et al., 2010).

Forest managers and downstream water users are often concerned with maximizing groundwater recharge at the end of the snowmelt period in forested areas (Ffolliott et al., 1989). Our results indicate that the increased NDSI following treatments also appeared to persist longer into the spring season. Over the winter season 2009–2010, NDSI in control and treatment units similarly fluctuated, likely due to temperature variations. Treated units had consistently greater NDSI throughout the winter season. Most importantly, at the end of the winter season by April 1, 2010, treated units had consistently greater NDSI compared to their control counterparts (Fig. 6). Persistent snow cover into the spring season is important for Arizona and across western North America, where decreases in annual April 1 snow-water equivalent (SWE) in snowpack (Brown, 2000; Mote, 2006), earlier snowmelt (Barnett et al., 2005; Clow, 2010), decreases in runoff (Stahl et al., 2010), and decreased summer low flows (Stewart, 2009) have been observed and are expected to accelerate in the coming decades.

Snowmelt duration can be altered via forest management (Ffolliott et al., 1989). The most persistent snow retention with the largest NDSI by April 1 was observed at the Centennial Forest B thin-and-burn site

with an average forest canopy cover of 24% and tree density of 7 trees/cell. Among the entire range of canopy cover of 22–51% found in the hyperspectral data, the canopy cover and forest structure at this site might represent the optimum threshold that the regional restoration efforts are seeking. Despite the adjacent proximity and similar key factors that influence snow accumulation, including snowfall, wind, and topographic slope and aspect, (Varhola et al., 2010), the 24% canopy cover site had the greatest NDSI value by April 1. Among many variables, forest canopy cover has been shown to be most highly correlated with snow accumulation and snowmelt (Varhola et al., 2010) and canopy cover decreases can lead up to 75–110% increase in snow accumulation (Varhola et al., 2010). Similar to this estimated increase in metadata analysis (Varhola et al., 2010), Fig. 8 indicates a significant increase in NDSI from 0.36 at the control site to 0.74 at the treated site by April 1. The optimum threshold is expected to create a balance between canopy cover versus canopy gap that reduces snow interception and sublimation by canopy, while providing enough shade. Much efforts are underway using ground-based investigations and process-based biophysical models to identify this threshold. Remote sensing-based, landscape-scale estimates complement such efforts.

5. Conclusion

Snow cover mapping in Arizona is a challenge due to the thin and patchy snow distribution. We find firstly that MOD10 product works well in estimating daily snow distribution and examining temporal trends in the daily snow record. Complementary to the ground-based snow measurements at SNOTEL point locations, the spatially-explicit regional-scale MODIS data provides an ideal dataset for the dynamic snow cover in Arizona that accumulates and rapidly melts within only a few days. Landsat-derived binary classification of snow presence and absence, however, does not perform well despite its higher spatial resolution, but likely due to its coarser temporal resolution. These findings suggest that temporal resolution in satellite data might be more important for future efforts in mapping snow distribution in Arizona than spatial resolution. Secondly, Landsat NDSI performs well at our local study area and effectively estimates the forest management effects on snow accumulation and retention, a previously undocumented trend with satellite data. Thirdly, using fine-resolution hyperspectral data, we find that optimum forest canopy cover can be achieved via forest restoration for increased snow accumulation and retention. We demonstrate that forest restoration efforts have significantly increased snow accumulation and retention into the spring season potentially contributing to improved water storage and harvest, while reducing catastrophic wildfire hazards.

Acknowledgments

References

Abatzoglou, J. T. (2011). Influence of the PNA on declining mountain snowpack in the Western United States. *International Journal of Climatology*, 1135–1142.

Adam, J. C., Hamlet, A. F., & Lettenmaier, D. P. (2009). Implications of global climate change for snowmelt hydrology in the twenty-first century. *Hydrological Processes*, *23*, 962–972.

Andreadis, K. M., Storck, P., & Lettenmaier, D. P. (2009). Modeling snow accumulation and ablation processes in forested environments. *Water Resources Research*, *45*.

Arizona Department of Water Resources (ADWR) (2010). *Upper San Pedro Water District comprehensive water resources plan, 17.*

Arsenault, K. R., Houser, P. R., & De Lannoy, G. J. (2012). Evaluation of the MODIS snow cover fraction product. *Hydrological Processes*, *28*, 980–998.

Ashfaq, M., Ghosh, S., Kao, S. C., Bowling, L. C., Mote, P., Touma, D., ... Diffenbaugh, N. S. (2013). Near-term acceleration of hydroclimatic change in the Western US. *Journal of Geophysical Research: Atmospheres*, *118*, 10–676.

Balice, R. G., Miller, J. D., Oswald, B. P., Edminister, C., & Yool, S. R. (2000). *Forest surveys and wildfire assessment in the Los Alamos; 1998–1999. Los Alamos, NM: USA Los Alamos National Laboratory, 12 (LA–13714–MS).*

Barnett, T. P., Adam, J. C., & Lettenmaier, D. P. (2005). Potential impacts of a warming climate on water availability in snow-dominated regions. *Nature*, *438*, 303–309.

Besic, N., Vasile, G., Gottardi, F., Gailhard, J., Girard, A., & d'Urso, G. (2014). Calibration of a distributed SWE model using MODIS snow cover maps and in situ measurements. *Remote Sensing Letters*, *5*, 230–239.

Brown, R. D. (2000). Northern Hemisphere snow cover variability and change, 1915–97. *Journal of Climate*, *13*, 2339–2355.

Brown, R. D., & Mote, P. W. (2009). The response of Northern Hemisphere snow cover to a changing climate. *Journal of Climate*, *22*, 2124–2145.

Brutel-Vuilmet, C., Ménégoz, M., & Krinner, G. (2013). An analysis of present and future seasonal Northern Hemisphere land snow cover simulated by CMIP5 coupled climate models. *The Cryosphere*, *7*, 67–80.

Cayan, D. R. (1996). Interannual climate variability and snowpack in the Western United States. *Journal of Climate*, *9*, 928–948.

Cayan, D. R., Redmond, K. T., & Riddle, L. G. (1999). ENSO and hydrologic extremes in the Western United States. *Journal of Climate*, *12*, 2881–2893.

Chokmani, K., Dever, K., Bernier, M., Gauthier, Y., & Paquet, L. M. (2010). Adaptation of the SNOWMAP algorithm for snow mapping over eastern Canada using Landsat-TM imagery. *Hydrological Sciences Journal–Journal des Sciences Hydrologiques*, *55*, 649–660.

Christensen, N. S., Wood, A. W., Voisin, N., Lettenmaier, D. P., & Palmer, R. N. (2004). The effects of climate change on the hydrology and water resources of the Colorado River basin. *Climatic Change*, *62*, 337–363.

Clow, D. W. (2010). Changes in the timing of snowmelt and streamflow in Colorado: A response to recent warming. *Journal of Climate*, *23*, 2293–2306.

Czerwinski, C. J., King, D. J., & Mitchell, S. W. (2014). Mapping forest growth and decline in a temperate mixed forest using temporal trend analysis of Landsat imagery, 1987–2010. *Remote Sensing of Environment*, *141*, 188–200.

Czyzowska-Wisniewski, E. H., van Leeuwen, W. J., Hirschboeck, K. K., Marsh, S. E., & Wisniewski, W. T. (2015). Fractional snow cover estimation in complex alpine-forested environments using an artificial neural network. *Remote Sensing of Environment*, *156*, 403–417.

de Jong, R., de Bruin, S., de Wit, A., Schaepman, M. E., & Dent, D. L. (2011). Analysis of monotonic greening and browning trends from global NDVI time-series. *Remote Sensing of Environment*, *115*, 692–702.

Dettinger, M. D., Cayan, D. R., Diaz, H. F., & Meko, D. M. (1998). North–south precipitation patterns in western North America on interannual-to-decadal timescales. *Journal of Climate*, *11*, 3095–3111.

Dietz, A. J., Kuenzer, C., Gessner, U., & Dech, S. (2012). Remote sensing of snow — A review of available methods. *International Journal of Remote Sensing*, *33*, 4094–4134.

Dore, S., Kolb, T. E., Montes-Helu, M., Eckert, S. E., Sullivan, B. W., Hungate, B. A., ... Finkral, A. (2010). Carbon and water fluxes from ponderosa pine forests disturbed by wildfire and thinning. *Ecological Applications*, *20*, 663–683.

Dore, S., Montes-Helu, M., Hart, S. C., Hungate, B. A., Koch, G. W., Moon, J. B., ... Kolb, T. E. (2012). Recovery of ponderosa pine ecosystem carbon and water fluxes from thinning and stand-replacing fire. *Global Change Biology*, *18*, 3171–3185.

Dozier, J. E. F. F. (1984). Snow reflectance from Landsat-4 thematic mapper. *IEEE Transactions on Geoscience and Remote Sensing*, *3*, 323–328.

Dozier, J. (1989). Spectral signature of alpine snow cover from the Landsat Thematic Mapper. *Remote Sensing of Environment*, *28*, 9–22.

Dye, D. G. (2002). Variability and trends in the annual snow-cover cycle in Northern Hemisphere land areas, 1972–2000. *Hydrological Processes*, *16*, 3065–3077.

Eastman, R. J., Sangermano, F., Ghimire, B., Zhu, H., Chen, H., Neeti, N., ... Crema, S. C. (2009). Seasonal trend analysis of image time series. *International Journal of Remote Sensing*, *30*, 2721–2726.

Ffolliott, P. F., Gottfried, G. J., & Baker, M. B. (1989). Water yield from forest snowpack management: Research findings in Arizona and New Mexico. *Water Resources Research*, *25*, 1999–2007.

Ffolliott, P. F., & Baker, M. B., Jr. (2000). Snowpack hydrology in the southwestern United States: Contributions to watershed management. *Land Stewardship in the 21st Century: The Contributions of Watershed Management. Proceedings RMRS-P-13.* (pp. 274–276). USDA Forest Service.

Finkral, A. J., & Evans, A. M. (2008). The effects of a thinning treatment on carbon stocks in a northern Arizona ponderosa pine forest. *Forest Ecology and Management*, *255*, 2743–2750.

Gafurov, A., & Bárdossy, A. (2009). Snow cover data derived from MODIS for water balance applications. *Hydrology and Earth System Sciences Discussions*, *6*, 791–841.

Gao, J., Williams, M. W., Fu, X., Wang, G., & Gong, T. (2012). Spatiotemporal distribution of snow in eastern Tibet and the response to climate change. *Remote Sensing of Environment*, *121*, 1–9.

Gottfried, G. J., & Ffolliott, P. F. (1980). Evaluation of snowmelt lysimeters in an Arizona mixed conifer stand. *Hydrological and Water Resources in Arizona and Southwest*, *10*, 221–229.

Hall, D. K., Foster, J. L., Chien, J. Y., & Riggs, G. A. (1995). Determination of actual snow-covered area using Landsat TM and digital elevation model data in Glacier National Park, Montana. *Polar Record*, *31*, 191–198.

Hall, D. K., Foster, J. L., Salomonson, V. V., Klein, A. G., & Chien, J. Y. L. (2001a). Development of a technique to assess snow-cover mapping errors from space. *IEEE Transactions on Geoscience and Remote Sensing*, *39*, 432–438.

Hall, D. K., Riggs, G. A., Salomonson, V. V., Barton, J. S., Casey, K., Chien, J. Y. L., ... Tait, A. B. (2001b). *Algorithm theoretical basis document (ATBD) for the MODIS snow and sea ice-mapping algorithms*. NASA GSFC (September).

Hall, D. K., Riggs, G. A., & Salomonson, V. V. (2006). MODIS snow and sea ice products. *Earth science satellite remote sensing* (pp. 154–181). Berlin Heidelberg: Springer.

Hall, D. K., & Riggs, G. A. (2007). Accuracy assessment of the MODIS snow products. *Hydrological Processes*, *21*, 1534–1547.

Hancock, S., Baxter, R., Evans, J., & Huntley, B. (2013). Evaluating global snow water equivalent products for testing land surface models. *Remote Sensing of Environment, 128*, 107–117.

Harpold, A., Brooks, P., Rajagopal, S., Heidbuchel, I., Jardine, A., & Stielstra, C. (2012). Changes in snowpack accumulation and ablation in the intermountain west. *Water Resources Research, 48*.

Harpold, A., & Molotch, N. P. (2013). December Investigating snowmelt infiltration dynamics in the Western US using the SNOTEL network. *AGU Fall Meeting Abstracts, vol. 1*. (pp. 1347).

Hedstrom, N. R., & Pomeroy, J. W. (1998). Measurements and modelling of snow interception in the boreal forest. *Hydrological Processes, 12*, 1611–1625.

Heffelfinger, S. (2012). *A field investigation on the impacts of forest thinning on snowpack accumulation in ponderosa pine forests of Northern Arizona.* (M.S. Thesis) Northern Arizona University.

Helsel, D., & Hirsch, R. (2002). Statistical methods in water resources. *Techniques of water-resources investigations of the United States Geological Survey. Book 4, Hydrologic analysis and interpretation. Chapter A3.* (pp. 1–524). US Geological Survey.

Hidalgo, H. G., Das, T., Dettinger, M. D., Cayan, D. R., Pierce, D. W., Barnett, T. P., ... Nozawa, T. (2009). Detection and attribution of streamflow timing changes to climate change in the Western United States. *Journal of Climate, 22*, 3838–3855.

Huang, X., Liang, T., Zhang, X., & Guo, Z. (2011). Validation of MODIS snow cover products using Landsat and ground measurements during the 2001–2005 snow seasons over northern Xinjiang, China. *International Journal of Remote Sensing, 32*, 133–152.

Intergovernmental Panel on Climate Change (IPCC) (2013). Climate change 2013: The physical science basis. *Contribution of working group I to the fifth assessment report of the Intergovernmental Panel on Climate Change.*

Jardine, A., Merideth, R., Black, M., & LeRoy, S. (2013). *Assessment of climate change in the southwest United States: A report prepared for the National Climate Assessment.* Island press.

Kapnick, S. B., & Delworth, T. L. (2013). Controls of global snow under a changed climate. *Journal of Climate, 26*, 5537–5562.

Kendall, M. G. (1948). *Rank correlation methods.*

Klein, A. G., Hall, D. K., & Riggs, G. A. (1998). Improving snow cover mapping in forests through the use of a canopy reflectance model. *Hydrological Processes, 12*, 1723–1744.

Knowles, N., Dettinger, M. D., & Cayan, D. R. (2006). Trends in snowfall versus rainfall in the Western United States. *Journal of Climate, 19*, 4545–4559.

Kolb, T. E., Breshears, D., Montes-Helu, M., & Flikkema, P. (2009). Impacts of forest thinning on water balance. *Final report to Arizona Water Institute on project AWI–08–23* (pp. 13).

Li, Z., & Guo, X. (2012). Detecting climate effects on vegetation in northern mixed prairie using NOAA AVHRR 1-km time-series NDVI data. *Remote Sensing, 4*, 120–134.

López-Moreno, J. I., Beniston, M., & García-Ruiz, J. M. (2008). Environmental change and water management in the Pyrenees: Facts and future perspectives for Mediterranean mountains. *Global and Planetary Change, 61*, 300–312.

Lundberg, A., & Halldin, S. (2001). Snow interception evaporation. Review of measurement techniques, processes, and models. *Theoretical and Applied Climatology, 70*(1–4), 117–133.

Lundberg, A., Nakai, Y., Thunehed, H., & Halldin, S. (2004). Snow accumulation in forests from ground and remote-sensing data. *Hydrological Processes, 18*, 1941–1955.

Lute, A. C., & Abatzoglou, J. T. (2014). Role of extreme snowfall events in interannual variability of snowfall accumulation in the Western United States. *Water Resources Research, 50*, 2874–2888.

Maher, A. I., Treitz, P. M., & Ferguson, M. A. (2012). Can Landsat data detect variations in snow cover within habitats of Arctic ungulates? *Wildlife Biology, 18*, 75–87.

Mann, H. B. (1945). Nonparametric tests against trend. *Econometrica: Journal of the Econometric Society*, 245–259.

Marchane, A., Jarlan, L., Hanich, L., Boudhar, A., Gascoin, S., Tavernier, A., ... Berjamy, B. (2015). Assessment of daily MODIS snow cover products to monitor snow cover dynamics over the Moroccan Atlas mountain range. *Remote Sensing of Environment, 160*, 72–86.

Mastin, M. C., Chase, K. J., & Dudley, R. W. (2011). Changes in spring snowpack for selected basins in the United States for different climate-change scenarios. *Earth Interactions, 15*, 1–18.

McCabe, G. J., & Dettinger, M. D. (2002). Primary modes and predictability of year-to-year snowpack variations in the Western United States from teleconnections with Pacific Ocean climate. *Journal of Hydrometeorology, 3*, 13–25.

McDowell, N. G., Adams, H. D., Bailey, J. D., Hess, M., & Kolb, T. E. (2006). Homeostatic maintenance of ponderosa pine gas exchange in response to stand density changes. *Ecological Applications, 16*, 1164–1182.

Metsämäki, S., Vepsäläinen, J., Pulliainen, J., & Sucksdorff, Y. (2002). Improved linear interpolation method for the estimation of snow-covered area from optical data. *Remote Sensing of Environment, 82*, 64–78.

Molotch, N. P., Colee, M. T., Bales, R. C., & Dozier, J. (2005). Estimating the spatial distribution of snow water equivalent in an alpine basin using binary regression tree models: The impact of digital elevation data and independent variable selection. *Hydrological Processes, 19*, 1459–1479.

Mote, P. W., Hamlet, A. F., Clark, M. P., & Lettenmaier, D. P. (2005). *Declining mountain snowpack in Western North America.*

Mote, P. W. (2006). Climate-driven variability and trends in mountain snowpack in Western North America. *Journal of Climate, 19*, 6209–6220.

Murphy, K. W., & Ellis, A. W. (2014). An assessment of the stationarity of climate and stream flow in watersheds of the Colorado River Basin. *Journal of Hydrology, 509*, 454–473.

Nakai, Y. (1996). *An observational study on evaporation from intercepted snow on forest canopies.* (Doctoral dissertation) Kyoto University.

Natural Resource Conservation Service (2015). http://www.wcc.nrcs.usda.gov/snow/snotel-wedata.html

National Snow and Ice Data Center (2015). http://nsidc.org/data/mod10a1

Neeti, N., & Eastman, J. R. (2011). A contextual Mann–Kendall approach for the assessment of trend significance in image time series. *Transactions in GIS, 15*, 599–611.

Neeti, N., Rogan, J., Christman, Z., Eastman, J. R., Millones, M., Schneider, L., ... Ghimire, B. (2012). Mapping seasonal trends in vegetation using AVHRR-NDVI time series in the Yucatán Peninsula, Mexico. *Remote Sensing Letters, 3*, 433–442.

Nolin, A. W. (2010). Recent advances in remote sensing of seasonal snow. *Journal of Glaciology, 56*, 1141–1150.

Painter, T. H., Rittger, K., McKenzie, C., Slaughter, P., Davis, R. E., & Dozier, J. (2009). Retrieval of subpixel snow covered area, grain size, and albedo from MODIS. *Remote Sensing of Environment, 113*, 868–879.

Peng, S., Piao, S., Ciais, P., Friedlingstein, P., Zhou, L., & Wang, T. (2013). Change in snow phenology and its potential feedback to temperature in the Northern Hemisphere over the last three decades. *Environmental Research Letters, 8*, 014008.

Pu, Z., Xu, L., & Salomonson, V. V. (2007). MODIS/Terra observed seasonal variations of snow cover over the Tibetan Plateau. *Geophysical Research Letters, 34*.

Riggs, G. A., Hall, D. K., & Salomonson, V. V. (2006). *MODIS snow products user guide to collection 5.* Digital Media, 80.

Rittger, K., Painter, T. H., & Dozier, J. (2013). Assessment of methods for mapping snow cover from MODIS. *Advances in Water Resources, 51*, 367–380.

Romanov, P., & Tarpley, D. (2007). Enhanced algorithm for estimating snow depth from geostationary satellites. *Remote Sensing of Environment, 108*, 97–110.

Salomonson, V. V., & Appel, I. (2004). Estimating fractional snow cover from MODIS using the normalized difference snow index. *Remote Sensing of Environment, 89*, 351–360.

Shreve, C. M., Okin, G. S., & Painter, T. H. (2009). Indices for estimating fractional snow cover in the western Tibetan Plateau. *Journal of Glaciology, 55*, 737–745.

Skov, K. R., Kolb, T. E., & Wallin, K. F. (2004). Tree size and drought affect ponderosa pine physiological response to thinning and burning treatments. *Forest Science, 50*, 81–91.

Stahl, K., Hisdal, H., Hannaford, J., Tallaksen, L., Van Lanen, H., Sauquet, E., ... Jordar, J. (2010). Streamflow trends in Europe: Evidence from a dataset of near–natural catchments. *Hydrology and Earth System Sciences, 14*, 2367.

Stewart, I. T. (2009). Changes in snowpack and snowmelt runoff for key mountain regions. *Hydrological Processes, 23*, 78–94.

Stoner, A. M. K., Hayhoe, K., & Wuebbles, D. J. (2009). Assessing general circulation model simulations of atmospheric teleconnection patterns. *Journal of Climate, 22*, 4348–4372.

Stroeve, J., Box, J. E., Gao, F., Liang, S., Nolin, A., & Schaaf, C. (2005). Accuracy assessment of the MODIS 16-day albedo product for snow: Comparisons with Greenland in situ measurements. *Remote Sensing of Environment, 94*, 46–60.

Sullivan, B. W., Kolb, T. E., Hart, S. C., Kaye, J. P., Dore, S., & Montes-Helu, M. (2008). Thinning reduces soil carbon dioxide but not methane flux from southwestern USA ponderosa pine forests. *Forest Ecology and Management, 255*, 4047–4055.

Svoma, B. M. (2011). El Niño–Southern Oscillation and snow level in the Western United States. *Journal of Geophysical Research: Atmospheres (1984–2012), 116*.

Teti, P. A. (2008). *Effects of overstory mortality on snow accumulation and ablation, vol. 2008*, Pacific Forestry Centre.

United States Department of Agriculture (USDA) (2013). *Draft environmental impact statement for the Four-Forest Restoration Initiative.* Coconino County, Arizona: Coconino and Kaibab National Forests.

Varhola, A., Coops, N., Bater, C. W., Teti, P., Boon, S., & Weiler, M. (2010). The influence of ground-and LiDAR-derived forest structure metrics on snow accumulation and ablation in disturbed forests. *Canadian Journal of Forest Research, 40*, 812–821.

Vogel, S. W. (2002). Usage of high-resolution Landsat 7 band 8 for single-band snow-cover classification. *Annals of Glaciology, 34*, 53–57.

Wang, X., Xie, H., & Liang, T. (2008). Evaluation of MODIS snow cover and cloud mask and its application in Northern Xinjiang, China. *Remote Sensing of Environment, 112*, 1497–1513.

Woods, S. W., Ahl, R., Sappington, J., & McCaughey, W. (2006). Snow accumulation in thinned lodgepole pine stands, Montana, USA. *Forest Ecology and Management, 235*, 202–211.

Yue, S., & Wang, C. (2004). The Mann–Kendall test modified by effective sample size to detect trend in serially correlated hydrological series. *Water Resources Management, 18*, 201–218.